

Erosion behaviour of Fe-Cr-C alloys: Cast alloy versus coating

Bratislav RAJICIC ^{1,*}, Aleksandar MASLAREVIC ¹, Gordana BAKIC ¹, Vesna MAKSIMOVIC ²,
Milos B. DJUKIC ¹

¹ University of Belgrade, Faculty of Mechanical Engineering, Belgrade, Serbia

² University of Belgrade, "Vinča" Institute of Nuclear Sciences – National Institute of the Republic of Serbia, Belgrade, Serbia

*Corresponding author: brajicic@mas.bg.ac.rs

Keywords

erosion
wear
Fe-Cr-C alloys
high chromium cast irons
plasma transferred arc

History

Received: 28-04-2024
Revised: 05-06-2024
Accepted: 15-06-2024

Abstract


This research focuses on the erosion wear behaviour of two Fe-Cr-C alloys with similar chemical compositions obtained using different production methods. The first alloy belongs to the high chromium cast irons (HCCI). It was made by casting, after which the samples were heat treated by annealing. The second alloy in the form of the coating was applied by the plasma transferred arc (PTA) surface welding process at the substrate material (structural carbon steel). Damage to the components of industrial plants due to erosive and/or abrasive wear is a frequent cause of failure and outages of such systems. For this reason, and to bring the experimental research closer to real service conditions, an erosion test was performed at a gas blast sand facility with a high erodent speed of 90 m/s and a higher feed rate than standard erosion testing parameters recommended in ASTM G76 standard. Microstructural characterisation of all samples was done using a scanning electron microscope (SEM). The X-ray diffraction analysis (XRD) was used to identify the phases present. Similar erosion mechanisms were observed on all tested specimens, but coated samples (PTA alloy) had a lower mass loss during the erosion test compared to cast samples (HCCI alloy), i.e. they showed better erosion resistance.

1. Introduction

The erosive wear of materials in the stream of solid particles is one of the damage mechanisms of material that can cause premature failure of industrial plant components. It can also affect the decline of the structural integrity of individual components and the entire industrial system. For example, erosion by solid particles in thermal power plants that burn coal as fuel, i.e. due to the presence of highly erosive fly ash that occurs after burning coal, can represent a major problem during the operation of such industrial plants [1]. There are various methods of protecting critical components exposed to erosive and/or abrasive wear in such systems. As the most effective methods, those based on the principle of making the critical component from materials with

increased erosion resistance or applying a coating with high erosion resistance on the surfaces of the critical components were singled out [2,3]. Also, a careful techno-economic analysis represents an important factor when choosing a technical solution for protecting components from wear.

Alloys of the Fe-Cr-C type are materials characterised by good resistance to erosive and/or abrasive wear. The exceptional wear resistance of these alloys is due to the presence of a large number of hard carbides based on chromium (Cr) of the M_7C_3 , $M_{23}C_6$ and M_3C types in the tough material matrix [4,5]. Due to its excellent characteristics such as high hardness value, high melting temperature, excellent resistance to chemical corrosion and wear resistance, Cr carbides in such alloys are widely used [6,7]. The wear resistance characteristics of Fe-Cr-C type alloys largely depend on the morphology, orientation, volume, size and composition of these carbides. In addition to Cr, carbon (C) content also exhibits a

 This work is licensed under a Creative Commons Attribution-NonCommercial 4.0 International (CC BY-NC 4.0) license

pronounced influence on wear resistance [8-12]. Depending on the chemical composition and the crystallisation process, Fe-Cr-C alloys can be hypoeutectic, eutectic and hypereutectic [4,13,14]. High wear resistance and relatively low cost of Fe-Cr-C alloys are the main reasons for their wide usage as materials for protection against erosive and/or abrasive wear [15].

High chromium cast iron (HCCI), with a chromium content of 11–40 wt.% Cr and a carbon content of 2–3.6 wt.% C, also belongs to the wear resistant Fe-Cr-C alloys classified according to the ASTM A532 standard [16-18]. The carbides formed in HCCI alloys are also a function of Cr and C content, and the most frequently present carbides in these alloys are of M_7C_3 , $M_{23}C_6$ and M_3C types. The wear resistance of HCCI alloys is based on the presence of the eutectic carbide, i.e. it depends on the amount and type of carbides present in the material. Also, as the carbide volume fraction (CVF) in these alloys increases, their wear resistance increases. In addition, heat treatments (HT) of HCCI alloys are carried out to ensure an optimal ratio of high wear resistance and high ductility of the substrate.

Fe-Cr-C alloys can also be applied in the form of a coating by various welding processes: tungsten inert gas (TIG) welding, electron-beam welding, laser welding, plasma transferred arc (PTA) welding, etc. [19-21]. Recently, the PTA process stood out from the mentioned processes due to the optimal ratio between the quality of the applied coatings and their application costs. With the PTA process, it is possible to apply various erosion resistant coatings, like metal coatings [22], metal matrix composite coatings and ceramic coatings [23,24], onto numerous substrate materials.

This paper presents the results of an erosion test, carried out under the same test conditions, for two Fe-Cr-C alloys of similar chemical composition obtained using different production technologies [25,26]. The first alloy is HCCI with approximately 25 wt.% Cr, made by casting and heat treated afterwards, while the second alloy is a coating applied by the PTA process.

2. Experimental methods

2.1 Materials and procedure

The experiment in this research consists of erosion testing of samples made of two alloys. The first group of samples was made by casting from

HCCI alloy and after that, the samples were heat treated (hereinafter these samples are designated as HCCI-HT). The second group of samples was made by applying a PTA surface welding to produce a coating on structural carbon steel (hereinafter these samples are designated with PTA-C).

HCCI-HT samples with dimensions of approx. $120 \times 120 \times 10$ mm were made by casting in sand moulds, using an induction furnace Inductotherm of 500 KW with a capacity of 1000 kg/h and a casting temperature of 1460–1520 °C. After casting, the samples were heat treated by annealing (HCCI-HT) in a 120 KV heat treatment furnace CER KP90 with a working range of 0–1200 °C. The chemical composition of the HCCI-HT samples is shown in Table 1, while the parameters of the two-step heat treatment regime are shown in Table 2.

Table 1. Chemical composition of HCCI-HT samples

Element	Chemical composition, wt. %						
	C	Mn	Si	Ni	Cr	Mo	Fe
HCCI-HT	3.0	0.45	0.44	0.6	24.4	0.2	balance

Table 2. Parameters of heat treatment (HCCI-HT)

Parameter	First step	Second step
Heating temperature, °C	600	600 – 960
Heating rate, °C/h	60	60
Holding time, h	1	2
Furnace cooling, h	–	48

The PTA-C samples with dimensions of approx. $120 \times 120 \times 6$ mm were made by coating deposition on the substrate material which was a structural carbon steel S235 (EN 10025) using the PTA process. The filler material for making these samples was commercial brand powder EuTroLoy 16659, manufactured by Castolin Eutectic, with 50–150 μ m granulation. PTA-C samples were made by depositing the coating using a PTA EuTronic Gap 3001 DC device, manufactured by Castolin Eutectic. The following deposition parameters were used: welding current 95 A, electric arc voltage 27.5 V, shield gas type 95 % Ar + 5 % H_2 , main speed movement 0.11 mm/s and oscillation speed 7 mm/s. The coating deposition process was carried out continuously, without interruption, with an applied coating thickness of approx. 4 mm.

The coating deposition parameters were more intense to obtain a coating with a thickness of 4 mm in one pass. This means that the obtained

dilution percentage was unusually high for the PTA process (approx. 40 %). Table 3 shows the chemical composition of the substrate material and filler material [27], as well as the average composition of the coating, which was determined based on the dilution percentage.

Table 3. Chemical composition of PTA-C samples

Element	Chemical composition, wt. %						
	C	Mn	Si	Ni	Cr	Mo	Fe
Filler material	3.9	0.25	1.1	4.5	32.5	0.5	balance
S235	0.16	1.4	0.21	–	–	–	balance
PTA-C	2.4	0.71	0.74	2.7	19.5	0.3	balance

X-ray diffractometry (XRD) was used to determine the phase composition of the tested samples (HCCI-HT and filler material of PTA-C) using a Rigaku Ultima IV diffractometer, Rigaku Co. Ltd., by CuK α radiation ($\lambda = 1.5406 \text{ \AA}$). The imaging of the samples was performed in the range of diffraction angles 2θ from 10 to 100°, with a step of 2 °/min. Phase identification of the collected data was performed with the DiffracPlus program using the XRD peak identification database.

Samples were prepared using a standard procedure including cutting, wet grinding and polishing. Murakami reagent (10 g KOH + 10 g K₃Fe(CN)₆ + 100 ml H₂O) was used for etching HCCI-HT samples, while for deep etching of carbides reagent of 50 ml FeCl₃ + 20 ml HCl + 930 ml ethanol was used. A solution of picric acid in ethyl alcohol (4 % HCl + ethanol) was used to etch the PTA-C sample. Wet grinding, with SiC sandpaper of P80 – P1000 grit size was performed on the device Phoenix 4000, Buehler. Alumina (Al₂O₃) of 1 μm granulation, in water suspension, was used for final polishing.

Metallographic examinations of HCCI-HT samples were performed on a scanning electron microscope (FE-SEM) type TESCAN Mira3 KSMU, operating at 20 kV at different magnifications. The PTA-C sample was examined on a scanning electron microscope SEM JEOL JSM 5800LV, Tescan Vega 5130MM.

2.2 Erosion test

The erosion test was carried out according to the modified standard test method for conducting erosion tests by solid particle impingement using gas jets ASTM G76 [28]. Two samples of HCCI-HT and PTA-C alloys were tested with a particle velocity

of approx. 90 m/s, which is significantly higher than the recommendations according to the ASTM G76 standard. This modification was used to bring the experimental test conditions closer to the actual service conditions present in industrial plants. The mass loss of the tested samples was measured with an analytical balance type B5, E. Mettler, with a capacity of 2000 g and an accuracy of 0.001 g.

Table 4 shows the parameters of the erosion test, while the schematic view of the erosion testing installation is given in Figure 1 [29]. The particle impact velocity was determined by the double-disk method [30].

Table 4. Erosion test parameters

Parameter	Value
Type of erodent	Foundry quartz sand
Erodent granulation, mm	0.26
SiO ₂ content, wt. %	≥ 98.0
Impact velocity, m/s	90
Impact angle, °	45
Feed particle rate, g/min.	3000
Nozzle-sample distance, mm	370
Nozzle diameter, mm	9
Carrying gas	Air
Erosion test duration, s	600
Temperature, °C	22

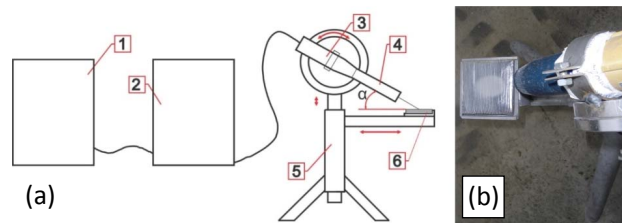


Figure 1. Device for solid particle erosion test: (a) scheme (1 – air compressor with pressure regulator; 2 – mixing chamber with particle tank; 3 – gun; 4 – nozzle; 5 – installation base; 6 – sample; α – impact angle), reprinted from Maslarević et al. [29], licensed under CC BY-NC-ND 4.0 and (b) macro photography

3. Results and discussion

For the HCCI-HT and PTA-C samples, based on the chemical composition shown in Tables 1 and 3, the eutectic temperature (T_E) and the carbide volume fraction (CVF) were determined according to Equations (1) and (2) [31,32]:

$$T_E = 1232 - 1929C + 351Cr, \quad (1)$$

$$CVF = 12.33C + 0.55Cr - 15.2. \quad (2)$$

Also, the carbon equivalent (C_{eq}) was determined for both alloys, according to Equation (3) [14], by which the alloys can be classified as hypoeutectic (< 4.3), eutectic ($= 4.3$) or hypereutectic (> 4.3):

$$C + 0.00474 Cr = C_{eq}. \quad (3)$$

Table 5 shows a comparative overview of the characteristic parameters for these two hypoeutectic alloys [25].

Table 5. Comparative parameters of the tested alloys

Parameter	HCCI-HT	PTA-C
C, %	3	2.4
Cr, %	24.4	19.5
T_E , °C	1260	1254
Cr/C	8.13	8.12
CVF, %	35.21	25.12
C_{eq} , %	3.12	2.49
Eutectic type	hypoeutectic	hypoeutectic

3.1 Microstructure of samples

Figure 2 shows the filler material (powder) used for the PTA-C sample. The spherical particles are mostly present since the atomization process is used during powder production [27]. The spheres mostly have a regular shape, they are compact, with pronounced dendritic structures and with partial microstructure porosity.

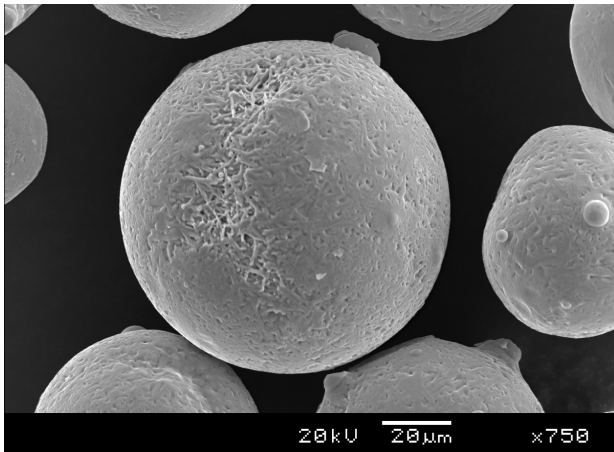


Figure 2. Filler material of PTA-C sample

XRD analysis of the phase composition of the HCCI-HT alloy samples shows that austenite (γ), martensite (M) and carbides of the M_7C_3 type are present in the microstructure of the sample (Fig. 3a). The presence of ferrite (α) or perlite (P) was not detected. In PTA-C samples, many chromium-based carbides of $Cr_{23}C_6$ and Cr_3C_2 type, as well as complex carbides of $Cr_2Fe_{14}C$ and M_7C_3 type, were identified in the powder composition (Fig. 3b) [26].

This can be expected considering the high content of Cr in this alloy.

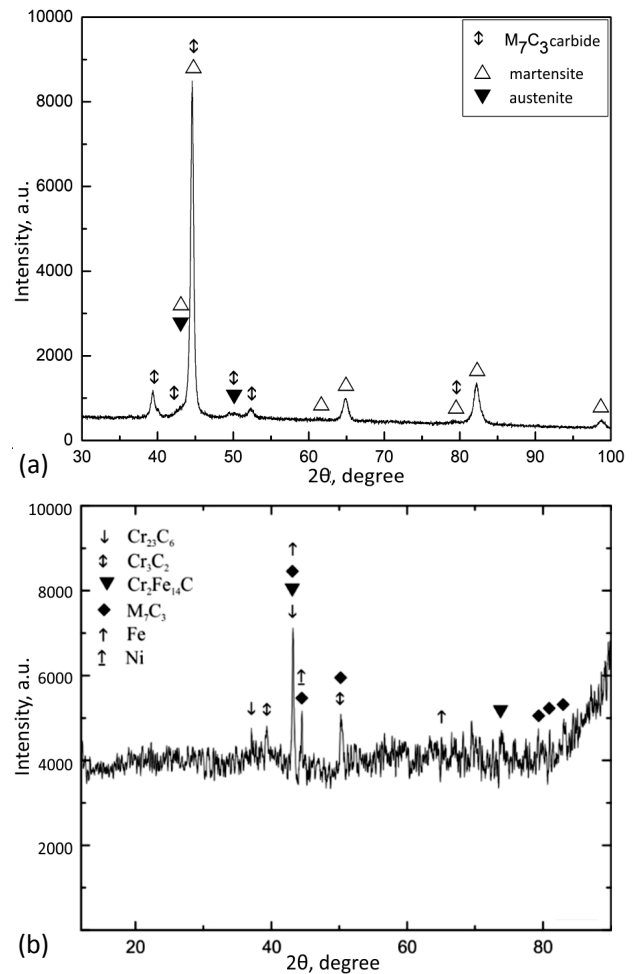


Figure 3. XRD patterns of: (a) HCCI-HT sample and (b) PTA-C filler material, reprinted from Maslarević [26], licensed under CC BY-NC-ND 4.0

Figure 4a shows the microstructure of the HCCI-HT sample obtained by SEM, where primary eutectic carbides and isolated secondary carbides of spheroidal and rod-shaped M_7C_3 type can be observed [2]. Figure 4b shows the microstructure of the PTA-C sample, also obtained by SEM. A homogeneous microstructure of the hypoeutectic alloy can be observed, which is austenitic dendritic with a eutectic phase. Austenitic dendrites have directed growth in the direction of heat transfer, normally in the direction of the coating-substrate bond layer. This was also observed by other authors [33]. The eutectic consists of a very fine carbide network in an austenite base, where very fine carbides are observed in the interdendritic region.

3.2 Erosion test results

The erosion test was performed on two samples made of HCCI-HT and PTA-C alloy. After

this test, a very similar elliptical shape of the eroded surface was observed on all samples (Fig. 5). The dimensions of the erosion zone in the HCCI-HT samples ranged from 100 – 110 × 80 – 90 mm (Fig. 5a). In the PTA-C sample, the dimensions of the central part of the erosion zone are in the range of 80 – 90 × 65 – 75 mm (Fig. 5b).

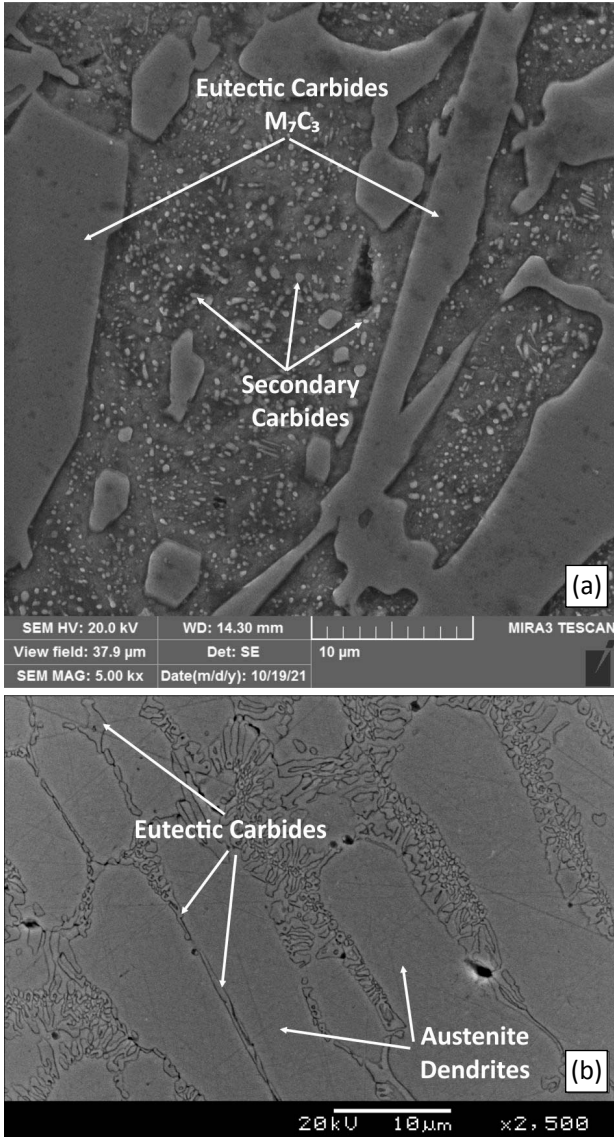


Figure 4. SEM micrographs of samples: (a) HCCI-HT, adapted from Rajcic et al. [2], copyrighted by Springer Nature and reproduced with permission from SNCSC and (b) PTA-C

The eroded surface of the PTA-C sample is slightly different compared to the HCCI-HT sample. This is due to the visible coating passes representing an additional obstacle to the flow of erosive particles during this test. Also, in the case of the PTA-C sample, pronounced local plastic deformation is observed in the middle of the erosion zone. This is a result of the uneven surface due to the coating passes.

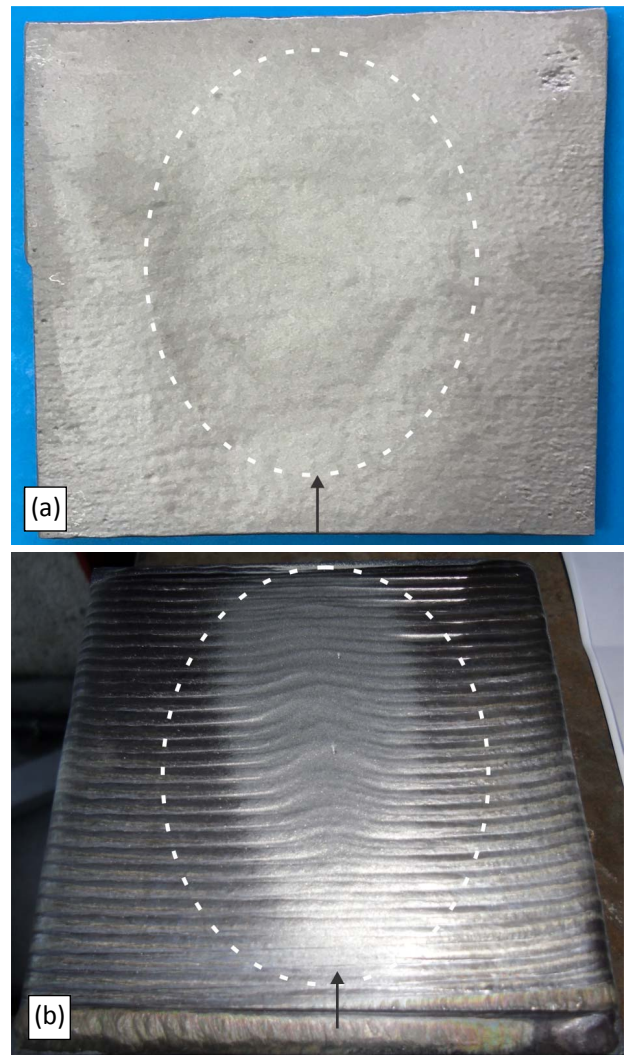


Figure 5. Eroded samples: (a) HCCI-HT and (b) PTA-C

The mass loss (Δm) of the erosion tested samples is shown in Figure 6 (SD – standard deviation), where it can be concluded that the PTA-C sample has better erosion resistance than the HCCI-HT sample.

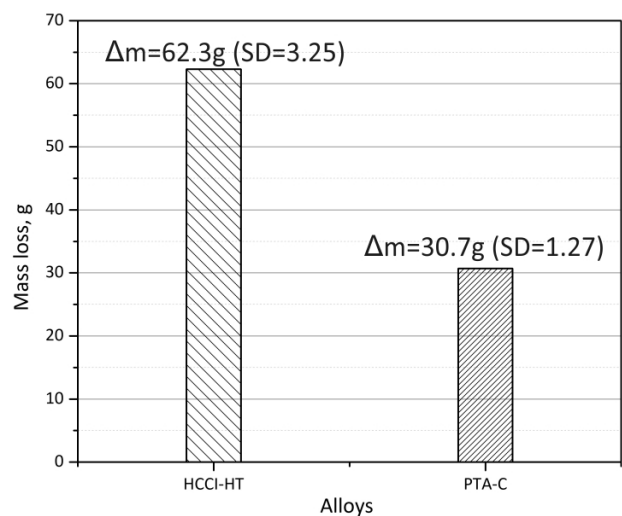


Figure 6. Erosion test results – mass loss Δm of tested alloys

3.3 Erosion mechanisms

Figure 7 shows the SEM microstructure of the eroded HCCI-HT sample. Various erosion wear mechanisms can be observed like cutting, scratching, rubbing marks and crater formation with carbide pulling out and lips formation during plastic deformation.

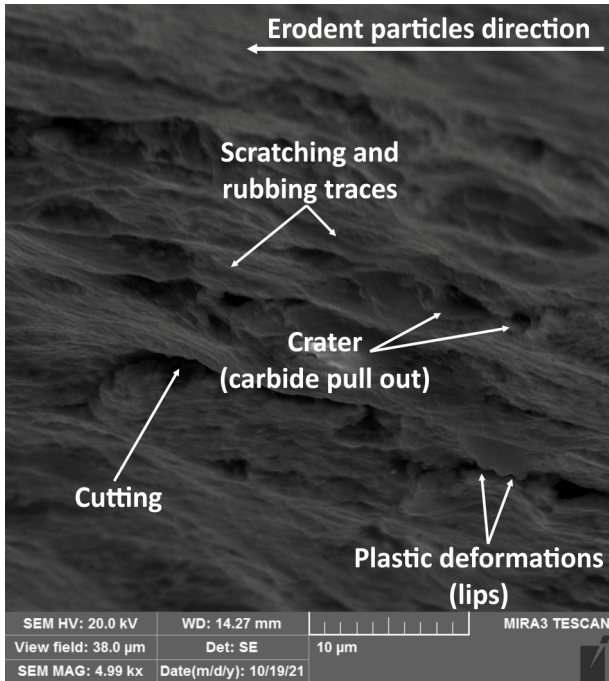


Figure 7. SEM micrographs of eroded surface morphology of HCCI-HT sample

The SEM microstructure of the PTA-C sample is shown in Figure 8. It can be concluded that this surface is also eroded by similar erosion wear mechanisms: cutting, crater formation with carbide pulling out and plastic deformation.

In the case of the HCCI-HT sample, there is a relatively large CVF of eutectic carbides. This, together with the base containing evenly distributed coarse primary and fine secondary carbides, represents a good obstacle for collisions with erodent particles. Also, microdefragmentation and breakage of primary eutectic carbides were observed in the HCCI-HT sample, which was also concluded by other authors in their research [34-36].

Although the erosion mechanisms for the HCCI-HT and PTA-C samples are very similar, the erosion resistance of the PTA-C samples is significantly higher. The primary reason for this is the size of the carbide phase. The carbides in the PTA-C alloy are much smaller than those in the HCCI-HT alloy. Also, they are much better bonded to the alloyed substrate material.

Therefore, defragmentation and breakage of carbides do not occur in PTA-C samples. Instead, entire carbides are removed (pulled out) from the

eutectic phase during the erosion test. Also, the better erosive resistance of the PTA-C alloy can be attributed to its changed eutectic morphology. Less elongated and less continuous eutectic carbides in this alloy further improve the erosion resistance of the PTA-C alloy [34-38].

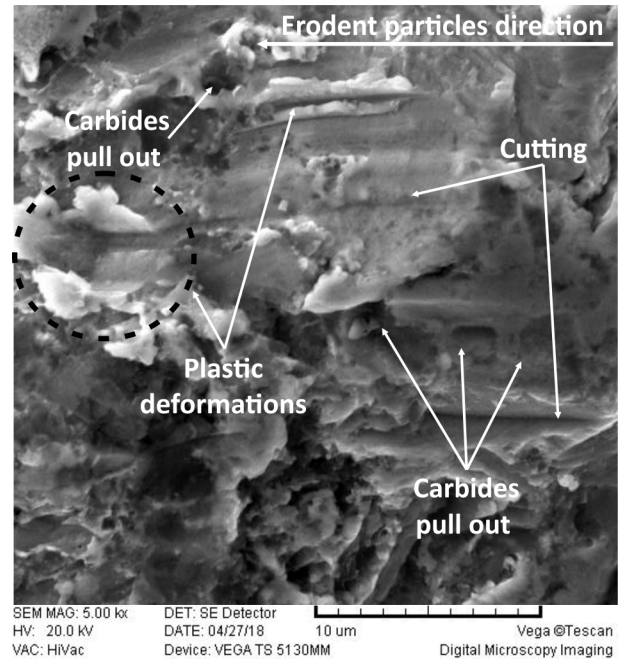


Figure 8. SEM micrographs of eroded surface morphology of PTA-C sample

Figure 9 schematically shows the cross-section of both samples during the erosion test, where the HCCI-HT alloy is shown in Figure 9a [2] and the PTA-C alloy in Figure 9b [25].

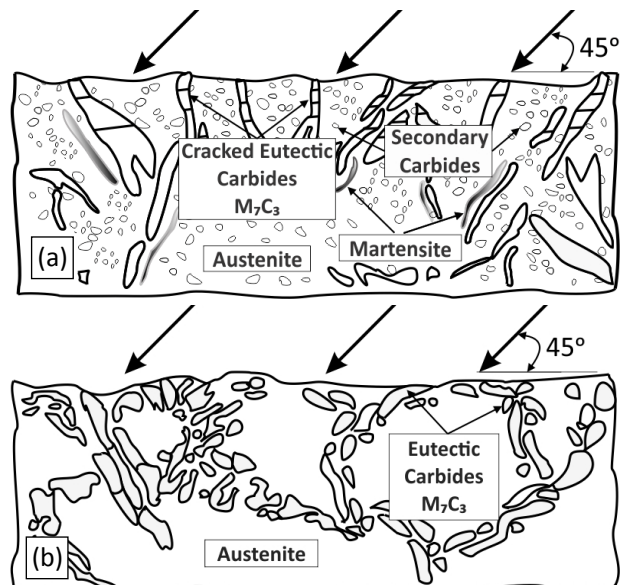


Figure 9. Cross-section of samples during erosion test: (a) HCCI-HT, adapted from Rajcic et al. [2], copyrighted by Springer Nature and reproduced with permission from SNCSC and (b) PTA-C, reprinted from Rajčić [25], licensed under CC BY-NC-ND 4.0

4. Conclusion

The erosion behaviour of two Fe-Cr-C alloys obtained by different methods with similar chemical compositions has been investigated. HCCI-HT samples were produced by casting and heat treated afterwards. The PTA-C samples were made using the PTA surface welding process for coating deposition. The main conclusions on the erosion behaviour of these samples are as follows.

Similar erosion mechanisms were observed at both examined samples (HCCI-HT and PTA-C), i.e. cutting, scratching and rubbing, craters formation with carbide pulling out, plastic deformation, etc.

PTA-C samples showed better erosion resistance than HCCI-HT samples, which resulted in less mass loss.

The main reason for the lower mass loss of PTA-C than HCCI-HT samples is the size of the carbide phase. The carbides in the PTA-C samples are much smaller than in the HCCI-HT sample. The carbides in the PTA-C sample are better bonded to the substrate material, which is additionally strengthened by alloying. Also, these carbides in the PTA-C sample are not defragmented and broken like in the HCCI-HT sample. Instead, whole carbides of small dimensions are pulled out from the eutectic phase.

On the other hand, knowing the technological process of coating, it can be concluded that the PTA process disadvantage is the impossibility of coating deposition on inaccessible parts of industrial components (e.g. on the inner surface of pipes, etc.), as well as on components with complex geometry.

Acknowledgement

This research was supported by the Ministry of Science, Technological Development and Innovation of the Republic of Serbia under the agreement on financing the scientific research work of teaching staff at accredited higher education institutions in 2024 (contract no. 451-03-65/2024-03/200105).

References

- [1] E. Raask, Tube erosion by ash impaction, *Wear*, Vol. 13, No. 4-5, 1969, pp. 301-315, DOI: [10.1016/0043-1648\(69\)90252-X](https://doi.org/10.1016/0043-1648(69)90252-X)
- [2] B.M. Rajcic, A. Maslarevic, G.M. Bakic, V. Maksimovic, M.B. Djukic, Erosion wear behavior of high chromium cast irons, *Transactions of the Indian Institute of Metals*, Vol. 76, No. 6, 2023, pp.1427-1437, DOI: [10.1007/s12666-022-02860-7](https://doi.org/10.1007/s12666-022-02860-7)
- [3] A. Maslarevic, G.M. Bakic, M.B. Djukic, B. Rajcic, V. Maksimovic, V. Pavkov, Microstructure and wear behavior of MMC coatings deposited by plasma transferred arc welding and thermal flame spraying processes, *Transactions of the Indian Institute of Metals*, Vol. 73, No. 1, 2020, pp. 259-271, DOI: [10.1007/s12666-019-01831-9](https://doi.org/10.1007/s12666-019-01831-9)
- [4] C. Fan, M.-C. Chen, C.-M. Chang, W. Wu, Microstructure change caused by (Cr,Fe)₂₃C₆ carbides in high chromium Fe-Cr-C hardfacing alloys, *Surface and Coatings Technology*, Vol. 201, No. 3-4, 2006, pp. 908-912, DOI: [10.1016/j.surfcoat.2006.01.010](https://doi.org/10.1016/j.surfcoat.2006.01.010)
- [5] S. Atamert, H.K.D.H. Bhadeshia, Microstructure and stability of Fe-Cr-C hardfacing alloys, *Materials Science and Engineering A*, Vol. 130, No. 1, 1990, pp. 101-111, DOI: [10.1016/0921-5093\(90\)90085-H](https://doi.org/10.1016/0921-5093(90)90085-H)
- [6] S. Loubière, C. Laurent, J.P. Bonino, A. Rousset, Elaboration, microstructure and reactivity of Cr₃C₂ powders of different morphology, *Materials Research Bulletin*, Vol. 30, No. 12, 1995, pp. 1535-1546, DOI: [10.1016/0025-5408\(95\)00123-9](https://doi.org/10.1016/0025-5408(95)00123-9)
- [7] M. Čekada, P. Panjan, M. Maček, P. Šmíd, Comparison of structural and chemical properties of Cr-based hard coatings, *Surface and Coatings Technology*, Vol. 151-152, 2002, pp. 31-35, DOI: [10.1016/S0257-8972\(01\)01582-1](https://doi.org/10.1016/S0257-8972(01)01582-1)
- [8] C.-M. Chang, L.-H. Chen, C.-M. Lin, J.-H. Chen, C.-M. Fan, W. Wu, Microstructure and wear characteristics of hypereutectic Fe-Cr-C cladding with various carbon contents, *Surface and Coatings Technology*, Vol. 205, No. 2, 2010, pp. 245-250, DOI: [10.1016/j.surfcoat.2010.06.021](https://doi.org/10.1016/j.surfcoat.2010.06.021)
- [9] Y.F. Zhou, Y.L. Yang, Y.W. Jiang, J. Yang, X.J. Ren, Q.X. Yang, Fe-24 wt.%Cr-4.1 wt.%C hardfacing alloy: Microstructure and carbide refinement mechanisms with ceria additive, *Materials Characterization*, Vol. 72, 2012, pp. 77-86, DOI: [10.1016/j.matchar.2012.07.004](https://doi.org/10.1016/j.matchar.2012.07.004)
- [10] G. Azimi, M. Shamanian, Effects of silicon content on the microstructure and corrosion behavior of Fe-Cr-C hardfacing alloys, *Journal of Alloys and Compounds*, Vol. 505, No. 2, 2010, pp. 598-603, DOI: [10.1016/j.jallcom.2010.06.084](https://doi.org/10.1016/j.jallcom.2010.06.084)
- [11] D. Turnbull, Phase changes, *Solid State Physics*, Vol. 3, 1956, pp. 225-306, DOI: [10.1016/S0081-1947\(08\)60134-4](https://doi.org/10.1016/S0081-1947(08)60134-4)
- [12] J.F. Flores, A. Neville, N. Kapur, A. Gnanavelu, Erosion-corrosion degradation mechanisms of Fe-Cr-C and WC-Fe-Cr-C PTA overlays in concentrated slurries, *Wear*, Vol. 267, No. 11, 2009, pp. 1811-1820, DOI: [10.1016/j.wear.2009.02.005](https://doi.org/10.1016/j.wear.2009.02.005)
- [13] L.-E. Svensson, B. Greftoft, B. Ulander, H.K.D.H. Bhadeshia, Fe-Cr-C hardfacing alloys for high-temperature applications, *Journal of Materials Science*, Vol. 21, No. 3, 1986, pp. 1015-1019, DOI: [10.1007/BF01117388](https://doi.org/10.1007/BF01117388)
- [14] L. Lu, H. Soda, A. McLean, Microstructure and mechanical properties of Fe-Cr-C eutectic

- composites, *Materials Science and Engineering A*, Vol. 347, No. 1-2, 2003, pp. 214-222, DOI: [10.1016/S0921-5093\(02\)00588-9](https://doi.org/10.1016/S0921-5093(02)00588-9)
- [15] S. Buytoz, M.M. Yildirim, H. Eren, Microstructural and microhardness characteristics of gas tungsten arc synthesized Fe-Cr-C coating on AISI 4340, *Materials Letters*, Vol. 59, No. 6, 2005, pp. 607-614, DOI: [10.1016/j.matlet.2004.08.038](https://doi.org/10.1016/j.matlet.2004.08.038)
- [16] G. Laird, R. Gundlach, K. Röhrig, *Abrasion-Resistant Cast Iron Handbook*, American Foundry Society, Des Plaines, 2000.
- [17] ASTM A532/A532M-10, Standard Specification for Abrasion-Resistant Cast Irons, 2023.
- [18] ISO 21988, Abrasion-Resistant Cast Irons – Classification, 2006.
- [19] Q.Y. Hou, Y.Z. He, Q.A. Zhang, J.S. Gao, Influence of molybdenum on the microstructure and wear resistance of nickel-based alloy coating obtained by plasma transferred arc process, *Materials & Design*, Vol. 28, No. 6, 2007, pp. 1982-1987, DOI: [10.1016/j.matdes.2006.04.005](https://doi.org/10.1016/j.matdes.2006.04.005)
- [20] M. Eroğlu, N. Özdemir, Tungsten-inert gas surface alloying of a low carbon steel, *Surface and Coatings Technology*, Vol. 154, No. 2-3, 2002, pp. 209-217, DOI: [10.1016/S0257-8972\(01\)01712-1](https://doi.org/10.1016/S0257-8972(01)01712-1)
- [21] R. Colaço, R. Vilar, Tribological properties of laser processed Fe-Cr-C alloys, *Materials Science Forum*, Vol. 473-474, 2005, pp. 53-58, DOI: [10.4028/www.scientific.net/MSF.473-474.53](https://doi.org/10.4028/www.scientific.net/MSF.473-474.53)
- [22] L. da Silva Ferreira, K. Graf, A. Scheid, Microstructure and properties of nickel-based C276 alloy coatings by PTA on AISI 316L and API 5L X70 steel substrates, *Materials Research*, Vol. 18, No. 1, 2015, pp. 212-221, DOI: [10.1590/1516-1439.332914](https://doi.org/10.1590/1516-1439.332914)
- [23] P.F. Mendez, N. Barnes, K. Bell, S.D. Borle, S.S. Gajapathi, S.D. Guest, H. Izadi, A. Kamyabi Gol, G. Wood, Welding processes for wear resistant overlays, *Journal of Manufacturing Processes*, Vol. 16, No. 1, 2014, pp. 4-25, DOI: [10.1016/j.jmapro.2013.06.011](https://doi.org/10.1016/j.jmapro.2013.06.011)
- [24] R.L. Deuis, J.M. Yellup, C. Subramanian, Metal-matrix composite coatings by PTA surfacing, *Composites Science and Technology*, Vol. 58, No. 2, 1998, pp. 299-309, DOI: [10.1016/S0266-3538\(97\)00131-0](https://doi.org/10.1016/S0266-3538(97)00131-0)
- [25] B.M. Rajičić, Materijali povećane erozije otpornosti izloženi ekstremnim uslovima rada na termoenergetskim postrojenjima [Materials with increased erosion resistance exposed to extreme working conditions at thermal power plants], PhD thesis, University of Belgrade, Faculty of Mechanical Engineering, Belgrade, 2023 [in Serbian].
- [26] A.M. Maslarević, Savremene tehnologije nanošenja prevlaka i njihova potencijalna primena na termoenergetskim postrojenjima [Modern deposition technologies for coatings and their potential application in thermal power plants], PhD thesis, University of Belgrade, Faculty of Mechanical Engineering, Belgrade, 2018 [in Serbian].
- [27] Metal Powder EuTroLoy 16659 Datasheet, Castolin Gesellschaft, Vienna, 2005.
- [28] ASTM G76, Standard Test Method for Conducting Erosion Tests by Solid Particle Impingement Using Gas Jets, 2018.
- [29] A. Maslarević, G.M. Bakić, M.B. Đukić, B. Rajičić, V. Maksimović, Karakterizacija prevlake 316L nanote postupkom plazma navarivanja [Characterization of a coating 316L applied by plasma transferred arc], *Hemijska industrija*, Vol. 72, No. 3, 2018, pp. 139-147, DOI: [10.2298/HEMIND170928005M](https://doi.org/10.2298/HEMIND170928005M) [in Serbian].
- [30] A.W. Ruff, L.K. Ives, Measurement of solid particle velocity in erosive wear, *Wear*, Vol. 35, No. 1, 1975, pp. 195-199, DOI: [10.1016/0043-1648\(75\)90154-4](https://doi.org/10.1016/0043-1648(75)90154-4)
- [31] Ö.N. Doğan, J.A. Hawk, G. Laird II, Solidification structure and abrasion resistance of high chromium white irons, *Metallurgical and Materials Transactions A*, Vol. 28, No. 6, 1997, pp. 1315-1328, DOI: [10.1007/s11661-997-0267-3](https://doi.org/10.1007/s11661-997-0267-3)
- [32] F. Maratray, R. Usseglio-Nanot, Factors Affecting the Structure of Chromium and Chromium-Molybdenum White Irons, *Climax Molybdenum S.A.*, Paris, France, 1970.
- [33] K. Günther, J.P. Bergmann, D. Suchodoll, Hot wire-assisted gas metal arc welding of hypereutectic FeCrC hardfacing alloys: Microstructure and wear properties, *Surface and Coatings Technology*, Vol. 334, 2018, pp. 420-428, DOI: [10.1016/j.surfcoat.2017.11.059](https://doi.org/10.1016/j.surfcoat.2017.11.059)
- [34] M. Jokari-Sheshdeh, Y. Ali, S. Corujeira Gallo, W. Lin, J.D. Gates, Effect of Cr:Fe ratio on the mechanical properties of (Cr,Fe)₇C₃ ternary carbides in abrasion-resistant white cast irons, *Journal of Materials Science*, Vol. 58, No. 17, 2023, pp. 7504-7521, DOI: [10.1007/s10853-023-08461-z](https://doi.org/10.1007/s10853-023-08461-z)
- [35] J.J. Coronado, Effect of (Fe,Cr)₇C₃ carbide orientation on abrasion wear resistance and fracture toughness, *Wear*, Vol. 270, No. 3-4, 2011, pp. 287-293, DOI: [10.1016/j.wear.2010.10.070](https://doi.org/10.1016/j.wear.2010.10.070)
- [36] J.J. Coronado, Effect of load and carbide orientation on abrasive wear resistance of white cast iron, *Wear*, Vol. 270, No. 11-12, 2011, pp. 823-827, DOI: [10.1016/j.wear.2011.02.009](https://doi.org/10.1016/j.wear.2011.02.009)
- [37] V. Heino, M. Kallio, K. Valtonen, V.-T. Kuokkala, The role of microstructure in high stress abrasion of white cast irons, *Wear*, Vol. 388-389, 2017, pp. 119-125, DOI: [10.1016/j.wear.2017.04.029](https://doi.org/10.1016/j.wear.2017.04.029)
- [38] J.D. Gates, G.J. Gore, *Wear of metals: Philosophies and practicalities*, *Materials Forum*, Vol. 19, 1995, pp. 53-89.